

## Accelerated Life Cycle Analysis of Lithium-Ion-Batteries under Different Fast-charging Algorithms

Simeon Kremzow-Tennie, Tobias Scholz, Friedbert Pautzke

*Electric Vehicle Institute, University of Applied Sciences Bochum, Germany. E-mail: simeon.kremzow-tennie@hs-bochum.de, tobias.scholz@hs-bochum.de, friedbert.pautzke@hs-bochum.de*

Kai André Boehm

*Esslingen University, Germany. E-mail: andre.boehm@hs-esslingen.de*

Benedikt Schmuelling

*Chair of Electric Mobility and Energy Storage Systems, University of Wuppertal, Germany. E-mail: schmuelling@uni-wuppertal.de*

Fast-charging is a relevant technical procedure required to further promote user acceptability of electric vehicles (EV), as well as the further decarbonization of mobility, as it allows to reduce charging times and range anxiety. However, fast-charging promotes accelerated battery aging and therefore limits the usability of the battery due to the reduction in lifetime. Based on this challenge, this research focuses on the analysis of different fast-charging algorithms to overcome the challenges of accelerated aging under fast-charging applications. Therefore, the classic boost-charging (BC) algorithm is compared against the standard constant current – constant voltage (CC-CV) algorithm and two anode potential based (APB) algorithms within the same testing framework. The results show that the maximum charging current used has a significant influence on the cycle life of the lithium-ion-batteries (LIBs) and all tested algorithms could not be performed to their full extent over the life-cycle-analysis (LCA) of the batteries. This was caused by safety relevant parameters, such as the end-of-charge (EOC) voltage that must not be overcome in order to operate the cell within the specified limits of the manufacturer.

*Keywords:* fast-charging, lithium-ion-battery, electric vehicle, boost-charging, life cycle analysis.

### 1. Introduction

Fast-charging LIBs is considered among the most important achievements in further promoting the market acceptance of EVs. With increasing regulations on combustion engine vehicles, personal and public transport require alternative drivetrain topologies. The most successful alternative drivetrain topology is the battery electric topology, which is available on vehicle models from nearly every manufacturer today. While the numbers of EVs are continuously increasing, the German governmental aim of 15 million electric vehicles by 2030 is considered not achievable judging the current situation (“Germany Will Miss 2030 E-Car Target Due to Lack of Charging Points – Consultancy” 2022; Reuters 2022). A big concern to potential customers is the range anxiety (Bonges and Lusk 2016; Pevac 2020), that is caused by the missing widespread charging infrastructure and long

charging times. Potential customers tend to compare the charging time to the duration of refueling a combustion engine vehicle at a gas station. This becomes especially significant for customers who depend on their vehicles for commercial use. The overall goal for fast-charging EVs for personal transport, is to reach 80% State-of-Charge (SOC) within a charging time of 15 minutes. Fast-charging however, proposes several challenges for EV manufacturers, as an efficient battery thermal management is required, cell degradation promoted, and energy efficiency decreased (Liu et al. 2016; Abdel-Monem et al. 2017; Kremzow-Tennie et al. 2021). Based on these challenges, this research focuses on the comparison of different fast-charging algorithms in comparison to the widely adapted standard CC-CV charging algorithm.

## 2. Charging algorithms

The authors of this publication started researching fast-charging algorithms within a research project where the standard CC-CV fast-charging algorithm and two algorithms based on the estimated anode potential were compared (Hermann et al. 2019). This research however did not take a broader look at other suitable fast-charging algorithms, which is therefore further extended in this work. This section displays a variety of charging profiles that have been analyzed in this research. The aim was to identify their benefits in comparison to the fast-charging CC-CV algorithm, which is considered the industry standard for charging LIBs (Tomaszewska et al. 2019; Abdel-Monem et al. 2017; Gao et al. 2019).

### 2.1 Constant Current – Constant Voltage

The CC-CV fast-charging algorithm is among the fastest charging procedures, due to the long constant current phase which is performed until the EOC voltage is reached. After that, the procedure switches to a constant voltage (CV phase) charging phase, during which the charging current decreases proportionally to the difference between cell voltage, EOC voltage and internal resistance. When implemented correctly, the CC-CV algorithm prevents overcharging, thus resulting in a safe charging procedure. Furthermore, due to the decreasing charging current towards the end of the procedure the risk of lithium-plating is reduced, as the decreasing current quantity reduces the amount of positively charged lithium-ions accumulating at the negative electrode without directly intercalating into it, which is particularly beneficial in the case of high charge states. (Tomaszewska et al. 2019; Kremzow-Tennie et al. 2021)

### 2.2 Anode potential based fast-charging

The APB fast-charging was designed to keep the cells anode potential above 0 V, as a potential below this threshold significantly promotes lithium plating (Liu et al. 2016; Kremzow-Tennie et al. 2022; Tian et al. 2021). During fast-charging the anode potential can reach beyond this threshold due to the high charge current, which therefore needs to be regulated. Therefore, two different profiles were designed, that aim to keep the anode potential above 0 V during charging.

During the previous research of the authors, this profile had been tested and it was identified, that APB fast-charging needs to be designed using a carefully parameterized electrochemical cell model with data that is not available directly by the cell manufacturer and usually neither publicly (Hermann et al. 2019). This aggravates the application of this procedure due to the challenge of proper parameterization.

### 2.3 Boost-charging

The BC profile, which was originally presented by Notten in 2005, is a CC-CV profile with an advanced CV phase (Notten, Veld, and Beek 2005). This constant voltage, usually the same value as the EOC voltage, is applied to the fully discharged (0% SOC) battery. The charge current results from the difference between the applied voltage and the actual cell voltage divided by the internal resistance of the battery. The resulting high charge current, here referred to as boost phase, requires limiting to prevent the cell from suffering damage due to overcharging, as well as potentially dangerous temperature developments. Therefore, a current and time limit for the initial boost phase is required. With an increasing SOC level, the current will decrease as the difference between the actual cell voltage and the set EOC voltage also decreases. After the time limit of the initial CV phase has been reached, the algorithm switches to a lower current for the following CC phase until the EOC voltage is reached and the algorithm switches to the final CV phase. During the sole CV charging at the end of the procedure, the current will decrease until the cut-off current threshold is reached and charging will be stopped. The aim of this algorithm was based on the idea, that lithium-plating occurs mainly at higher SOC levels and high charging currents. Therefore, it was designed to use higher charging currents at lower SOC levels, so that the risk of lithium plating is reduced.

## 3. Methodology and presentation of results

This chapter presents the experimental setup for the different test series, so that a comparison is possible.

### 3.1 Design of experiment

For the metrological analysis of aging under fast-charging conditions, four Sony VTC6A 21700 cells were connected in series for each test and placed in a controlled climatic environment at 45 °C to ensure a lower internal resistance (Kremzow-Tennie et al. 2022; Trentadue et al. 2018). Furthermore, several global parameters such as the EOC and end-of-discharge (EOD) voltage in accordance with the manufacturer's datasheet were set and are shown in Table 1.

Table 1. Presentation of the relevant parameters of the cell manufacturer, as well as parameters chosen for the testing framework.

	Parameter	Symbol	Value
OEM	EOD	$U_{\min}$	2.5 V
	EOC	$U_{\max}$	4.2 V
	Max. charge current	$I_{CH\max}$	9 A
	Max. temperature	$T_{\max}$	60 °C
	Nominal capacity	$C_N$	4 Ah
Test	Ambient temperature	$T_{\text{Set}}$	45 °C
	Discharge current	$I_{DCH}$	1.5 A
EOT	Capacity	$SOH_C$	80 %
	Internal resistance	$SOH_R$	200 %

In order to reduce negative influences of improper reversible electric connections, the cells under test were welded together, thus reducing the contact resistances to a minimum. (Brand et al. 2015) The cells were charged to 80 % SOC of the initially measured capacity before cycling, using their respective charging algorithm. Discharging was performed down to 2.6 V at a discharge rate of 0.375 C or 1.5 A, which was chosen to reduce the negative impacts of discharging stress on the cells. The C-rate describes the charge or discharge rate, which charges or discharges the battery within one hour completely. A low discharge current ensures that the battery can be discharged to a low SOC without falling below the EOD. After 25 cycles a characterization procedure consisting of a capacity and internal resistance test was performed to obtain the values for the SOH determination and to reduce inhomogeneities due to the serial connection of the cells. (Scholz et al. 2021) The low cycle numbers between the characterization procedures were chosen to gain a precise understanding of the aging behavior under the extreme charging

conditions. For the analysis of the cell, several key parameters were chosen, ensuring a controlled test procedure as well as reproducible and comparable results. Two key health indicators were chosen, which are considered as standard aging indicators in the automotive industry and have a direct influence on a cells usability for automotive applications. (Guenther et al. 2021) The  $SOH_R$  characterizes the state of health in dependence on the internal resistance, whereas the  $SOH_C$  characterizes the state of health in dependence on the usable capacity of a cell. For each of the two parameters an end of life (EOL) threshold has been chosen, which if reached by a cell, indicates that it is not further usable for automotive applications. In case of the  $SOH_R$  an internal resistance of 200 % is considered the EOL threshold, whereas for the  $SOH_C$  a decrease of the usable capacity by 20% was considered the threshold until recently. (Zhu et al. 2021) During the time of this research project a  $SOH_C$  of 80 % was the norm, but it has since been adapted to 80 - 70 % by most vehicle manufacturers. (Canals Casals et al. 2022) This capacity decrease is based on the nominal capacity of the cell. This research however, defines an  $SOH_C$  of 80 % based on the initially measured capacity before cycling as the end of test (EOT) threshold. For the analysis of the internal resistance three SOC points were chosen, as the internal resistance is dependent on the SOC. The chosen levels are 20 %, 50 % and 80 % SOC, as these describe the cells resistance characteristics at key points and the range can be considered the most used in vehicle applications. (Kostopoulos, Spyropoulos, and Kaldellis 2020) As mentioned before the automotive industry considers an internal resistance increase of the traction battery by 100 % as an EOL condition. This results from the significantly greater power losses due to the rise in internal resistance, which cause greater voltage drops as well as greater temperatures during charging and discharging (Ecker et al. 2012; Kremzow-Tennie, Hellwig, and Pautzke 2020). Especially under the fast-charging condition, as well as high power output of the battery, the battery's thermal management system might face difficulties in dissipating the excess heat caused by the greater internal resistance.

### 3.2 Presentation of charging algorithms

For the analysis of the BC algorithm three different test series were designed, that aimed to charge the cell from 0 % to 80 % SOC within 900 s. Each of these test series implemented a different current limit for the initial boost phase of the BC algorithm. Furthermore, different time limits to keep the charge throughput comparable, as well as comparable to the test series of the authors previous publication, were set up. It is important to note that for all series the same EOC voltage of 4.2 V was implemented, and the charge current was reduced similar to a CV phase when the cell voltage reached this value. This was done to prevent the cell from overcharging and maintain it within the voltage limits given by the manufacturer.

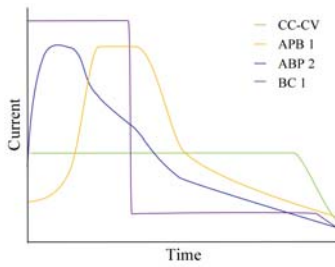


Fig. 1. Charge current profiles of the different analyzed charging algorithms

Fig. 1 presents the current profiles of the different charging algorithms that have been analyzed in this and the author's previous work. To improve readability, only one classic BC algorithm is shown, as the other two BC tests series have a similar profile, just with different current magnitudes and time limits. As visible in the figure, the BC algorithm behaves like a CC-CC-CV algorithm due to the implemented current limit.

#### 3.2.1 Boost-charge series 1

In BC series 1 a boost phase of 300 s with a charge current of 24 A was implemented, resulting in a SOC increase of around 50 % in relation to the initially capacity of 3.85 Ah at the end of the period. This was then followed by an 8 A CC phase for the remaining 600 s of charging time to achieve 80 % SOC within 900 s of overall charging time. The change in current profile over

the cycling period is shown in Fig. 2. The aging of the cells leads to a current reduction at the end of the boost phase at higher cycle numbers, since the EOD voltage was reached earlier.

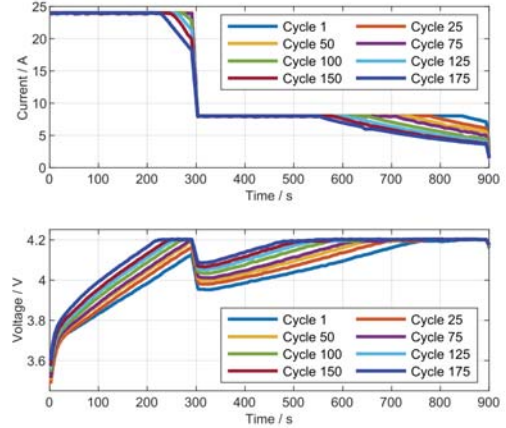


Fig. 2. Current and voltage profile of BC series 1

#### 3.2.2 Boost-charge series 2

For BC series 2, shown in Fig. 3, the boost phase was reduced to 240 s. The current was increased to 30 A, to achieve the goal of charging 50 % SOC within the boost period, which corresponds to a C-Rate of 7.5 C. The following CC phase was performed with a current of 6.82 A for the remaining 660 s.

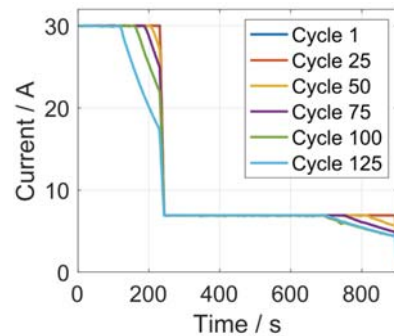


Fig. 3. Charge current profile of BC series 2

#### 3.2.3 Boost-charge series 3

In comparison to BC series 1, and 2, series 3 had the longest boost period and thus the lowest current at 18 A for 400 s. To still achieve 80 % SOC after 900 s, the following CC phase was performed at 9 A, as shown in Fig. 4.

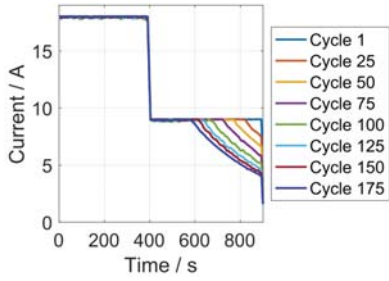


Fig. 4. Charge current profile of BC series 3

### 3.3 Discussion of results

For a reliable analysis of the SOH in dependence to the cells internal resistance and usable capacity, a characterization profile was performed after every 25 cycles. The results of these characterizations are presented in this chapter and are divided into the respective  $SOH_C$  and  $SOH_R$ .

#### 3.3.1 Internal resistance: $SOH_R$

To compare the internal resistance behavior for all three test-series and all three measured SOC the measured values are presented in Table 2. It is visible that internal resistance of test series 2, shows the highest overall resistance increase. For series 1 the worst performing cell has been labelled with the percentual increase values in Fig. 5. This was done as an example, as the worst performing cell of a module usually has the biggest impact on its overall performance. For test series 2 (Fig. 5) the internal resistance is showing the biggest increase at 20 % and 50 % SOC with in comparison to the other two series. This behavior is very likely to be caused by the high boost current. The high current is expected to cause a higher amounts of lithium plating, which results in the increase of the internal resistance. And while after 25 cycles no big difference between the internal resistance measurements of test series 1, 2, and 3 is visible, the difference in increase has become very visible after around 75 cycles. Here the increase is already above 8 % for test series 2, whereas test series 1 has an increase of 5.58 % and series 3 of 6.58 % as their respective average increases.

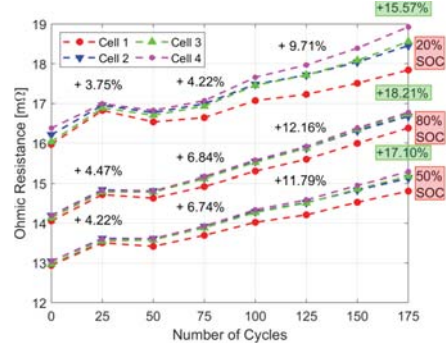


Fig. 5. Internal resistance values of BC series 1 with percentual increase label of the worst performing cell

In this test scenario, not only did the internal resistance increase the most, but it is also the series that stopped the earliest after 125 cycles.

Table 2. Average measured internal resistance for each BC series and the average increase in dependence to the cycle numbers

	Cycle	@ 20	@ 50	@ 80	Av. Incr.
		% SOC [mΩ]	% SOC [mΩ]	% SOC [mΩ]	
BC 1	25	16.913	13.570	14.793	4.38
	50	16.708	13.555	14.758	3.84
	75	16.908	13.858	15.085	5.58
	100	17.415	14.230	15.483	8.14
	125	17.655	14.458	15.838	9.68
	150	18.005	14.793	16.258	11.75
	175	18.445	15.100	16.638	13.73
BC 2	25	16.588	13.400	11.790	3.15
	50	17.350	14.110	12.202	7.33
	75	17.493	14.325	12.402	8.50
	100	18.440	15.085	13.106	13.23
	125	18.630	15.288	13.284	14.28
BC 3	25	16.365	13.268	14.438	2.84
	50	16.378	13.410	14.620	3.58
	75	16.875	13.853	15.105	6.58
	100	17.138	14.113	15.448	8.31
	125	17.583	14.465	15.875	10.65
	150	17.613	14.498	15.940	10.89
	175	17.860	14.668	16.238	12.20

#### 3.3.2 Usable capacity: $SOH_C$

The analysis of the discharged capacity of a traction battery is considered the most common



procedure of SOH analysis. To calculate the discharged capacity, the coulomb counting procedure was performed. As the discharge was always performed from the EOC voltage of 4.2 V (equivalent of 100 % SOC) until the EOD voltage was reached, it could be expected that the cell reached a SOC of close to 0%. The calculated reduction of usable capacity is shown in percentage labels of Fig. 6 as average values for BC series 1 as an example and the data of BC series 2 and 3 are given in Table 3.

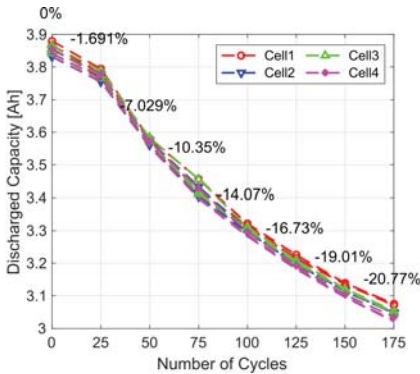


Fig. 6. Discharged capacity of BC series 1

Similar to the internal resistance, the spread between cells was the greatest in BC series 2, which is most likely caused by the faster aging due to the high current of the boost phase of test series 2. BC series 3 showed the least amount of spreading between the cells, which can be argued to be a result of the lowest boost current of all three series.

Table 3. Average percentual decrease of usable capacity measured during characterization.

Cycle	Capacity loss [%]		
	BC 1	BC 2	BC 3
25	1.69	5.49	5.35
50	7.03	10.11	8.73
75	10.35	13.86	11.91
100	14.07	17.86	14.37
125	16.73	20.21	16.83
150	19.01	-	18.51
175	20.77	-	20.52

Furthermore, series 2 reaches the EOT threshold for the SOH<sub>c</sub> of 80 % as the first series after just 125 cycles, as visible in Table 3. This underlines

the promoted aging due to the extremely high charge rate of 7.5 C or 30 A during the boost phase. Capacity loss of BC series 1 and 3 behave similar and both reached the EOT threshold after 175 cycles, thus lasting around 50 cycles longer due to the lower current during the boost phase.

### 3.3.3 Charged capacity during cycle testing

When analyzing the charged capacity during the BC cycles, it becomes visible that the originally designed BC algorithm cannot be performed throughout the full lifecycle of the batteries under test. This becomes especially visible in Fig. 2, where the current and voltage behavior of BC series 1 is shown. With increasing cycle numbers, the EOC voltage is reached before the BC period is finished, resulting in a decrease of charging current to prevent the cell from overcharging. Fig. 7 shows the difference between charged capacity during the BC phase in comparison to the CC-CV phase for each test series in dependence to the cycle number. Since BC series 2 reached the EOT after 125 cycles, it has the last appearance at cycle 100 in Fig. 7, where the boost phase is not able to charge the desired 50 % SOC anymore.

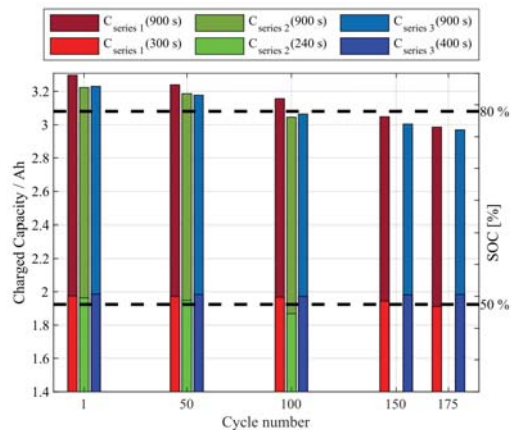


Fig. 7. Comparison of charged capacity for each test series, separated into BC and CC-CV phase

The other two BC algorithms are still able to charge the desired 50 %, but BC series 3 already fails to reach the desired 80 % SOC for the full 900 s of charging. It must be noted that the y-axis starts at 1.4 Ah so that the differences between the charged capacity during BC and the following CC-CV charging become more visible. The indications of 50 % and 80 % SOC on the right y-

axis are in dependence to the originally measured capacity of 3.85 Ah before the LCA was started.

## 5. Conclusion and outlook

Table 3 shows the cycle numbers at which the EOT threshold of 80 % SOH<sub>C</sub> had been reached. The CC-CV algorithm lasted 220 cycles (APB1 160 and APB2 180 cycles) until they reached the EOT, which can be explained by fact that the algorithm used the lowest current compared to the other test series. In general, it can be seen that for the BC algorithms the highest current results in the fastest aging, which is most likely caused by stronger lithium plating, as charging with the respective current was performed up to 50 % SOC. It has to be noted that all tested algorithms implemented significantly higher currents than the manufacturer allowed on cell level, which shows the implications of high energy cells when it comes to the application of fast-charging. The APB and BC algorithms have proven to allow for a similar cycle life, but the BC algorithm has the advantage of being implementable with parameters directly available from the manufacturer, which is not the case for the APB algorithm. However, all tested algorithms showed that the algorithm works for a new cell, but reaches its limits after a few cycles. This was already seen in the authors' previous publication for the CC-CV and APB algorithms and can also be seen for the BC algorithms of this publication, where for example in test series 2 (Fig. 3) the boost period of 240 s cannot be performed anymore after just 50 cycles. This further highlights the challenges of making fast-charging usable throughout the lifetime of a vehicle.

Overall, BC series 3 performed the best of the three tested series, as it was the only algorithm still able to charge 50 % SOC within the set boost phase even after 175 cycles. It can be seen that a careful consideration of the BC algorithm results in significant differences in cycle life, yet a more careful approach is suggested as the tested algorithms (BC 1,2, and 3) did not perform as good as the CC-CV algorithm of the previous work.

## Acknowledgement

The authors would like to thank the Federal Ministry for Economic Affairs and Climate Action for the funding of this research project within the Energy Program (BMWi.IIC6). Furthermore, the authors would like to thank the Bochum University of Applied Sciences for additional funding of parts of this work.

## References

- Abdel-Monem, Mohamed, Khiem Trad, Noshin Omar, Omar Hegazy, Peter Van den Bossche, and Joeri Van Mierlo. 2017. "Influence Analysis of Static and Dynamic Fast-Charging Current Profiles on Ageing Performance of Commercial Lithium-Ion Batteries." *Energy* 120 (February): 179–91. <https://doi.org/10.1016/j.energy.2016.12.110>
- Bonges, Henry A., and Anne C. Lusk. 2016. "Addressing Electric Vehicle (EV) Sales and Range Anxiety through Parking Layout, Policy and Regulation." *Transportation Research Part A: Policy and Practice* 83 (January): 63–73. <https://doi.org/10.1016/j.tra.2015.09.011>
- Brand, Martin J., Philipp A. Schmidt, Michael F. Zaeh, and Andreas Jossen. 2015. "Welding Techniques for Battery Cells and Resulting Electrical Contact Resistances." *Journal of Energy Storage* 1 (June): 7–14. <https://doi.org/10.1016/j.est.2015.04.001>
- Canals Casals, Lluc, Maite Etxandi-Santolaya, Pere Antoni Bibiloni-Mulet, Cristina Corchero, and Lluís Trilla. 2022. "Electric Vehicle Battery Health Expected at End of Life in the Upcoming Years Based on UK Data." *Batteries* 8 (10): 164. <https://doi.org/10.3390/batteries8100164>
- Ecker, Madeleine, Jochen B. Gerschler, Jan Vogel, Stefan Käbitz, Friedrich Hust, Philipp Dechent, and Dirk Uwe Sauer. 2012. "Development of a Lifetime Prediction Model for Lithium-Ion Batteries Based on Extended Accelerated Aging Test Data." *Journal of Power Sources* 215 (October): 248–57. <https://doi.org/10.1016/j.jpowsour.2012.05.012>
- Gao, Yizhao, Xi Zhang, Qiyu Cheng, Bangjun Guo, and Jun Yang. 2019. "Classification and Review of the Charging Strategies for Commercial Lithium-Ion Batteries." *IEEE Access* 7: 43511–24. <https://doi.org/10.1109/ACCESS.2019.2906117>
- "Germany Will Miss 2030 E-Car Target Due to Lack of Charging Points – Consultancy." 2022. *Clean Energy Wire*. June 29, 2022.

- <https://www.cleanenergywire.org/news/germany-will-miss-2030-e-car-target-due-lack-charging-points-consultancy>.
- Guenther, Lea Hannah, Tobias Scholz, Friedbert Pautzke, Heiko Fechtner, Benedikt Schmuelling, Nora Schelte, Semih Severengiz, Marcin Hinz, and Stefan Bracke. 2021. "Reliability Engineering of Electric Vehicle Powertrains: Data Collection and Analysis Based on Products in the Usage Phase." In *Proceedings of the 31st European Safety and Reliability Conference (ESREL 2021)*, 2573–80. Research Publishing Services. [https://doi.org/10.3850/978-981-18-2016-8\\_183-cd](https://doi.org/10.3850/978-981-18-2016-8_183-cd).
- Hermann, Pascal, Chunxi Zhang, Simeon Kremzow-Tennie, and Daniel Parzyszek. 2019. "Das Forschungsprojekt D-See [di: si:] – Durchgängiges Schnellladekonzept für Elektrofahrzeuge," 17.
- Kostopoulos, Emmanouil D., George C. Spyropoulos, and John K. Kaldellis. 2020. "Real-World Study for the Optimal Charging of Electric Vehicles." *Energy Reports* 6 (November): 418–26. <https://doi.org/10.1016/j.egy.2019.12.008>.
- Kremzow-Tennie, Simeon, Martin Hellwig, and Friedbert Pautzke. 2020. "A Study on the Influencing Factors Regarding Energy Consumption of Electric Vehicles." In *2020 21st International Conference on Research and Education in Mechatronics (REM)*, 1–6. Cracow, Poland: IEEE. <https://doi.org/10.1109/REM49740.2020.9313934>.
- Kremzow-Tennie, Simeon, Friedbert Pautzke, Haydar Mecit, Tobias Scholz, and Benedikt Schmuelling. 2021. "A Suggestion Towards Improving Electric Vehicle Fast Charging." In *Making Connected Mobility Work*, edited by Heike Proff, 251–61. Wiesbaden: Springer Fachmedien Wiesbaden. [https://doi.org/10.1007/978-3-658-32266-3\\_14](https://doi.org/10.1007/978-3-658-32266-3_14).
- Kremzow-Tennie, Simeon, Tobias Scholz, Friedbert Pautzke, Alexander Popp, Heiko Fechtner, and Benedikt Schmuelling. 2022. "A Comprehensive Overview of the Impacting Factors on a Lithium-Ion-Battery's Overall Efficiency." *Power Electronics and Drives* 7 (1): 9–28. <https://doi.org/10.2478/pead-2022-0002>.
- Liu, Qianqian, Chunyu Du, Bin Shen, Pengjian Zuo, Xinqun Cheng, Yulin Ma, Geping Yin, and Yunzhi Gao. 2016. "Understanding Undesirable Anode Lithium Plating Issues in Lithium-Ion Batteries." *RSC Advances* 6 (91): 88683–700. <https://doi.org/10.1039/C6RA19482F>.
- Notten, P.H.L., J.H.G. Op het Veld, and J.R.G. van Beek. 2005. "Boostcharging Li-Ion Batteries: A Challenging New Charging Concept." *Journal of Power Sources* 145 (1): 89–94. <https://doi.org/10.1016/j.jpowsour.2004.12.038>.
- Pevec, Dario. 2020. "A Survey-Based Assessment of How Existing and Potential Electric Vehicle Owners Perceive Range Anxiety." *Journal of Cleaner Production*, 12.
- Reuters. 2022. "German Transport Minister Reverses from 15 Mln Electric Vehicles Goal." *Reuters*, January 17, 2022, sec. Europe. <https://www.reuters.com/world/europe/german-transport-minister-reverses-15-mln-electric-vehicles-goal-2022-01-17/>.
- Scholz, Tobias, Simeon Kremzow-Tennie, Friedbert Pautzke, Heiko Fechtner, Alexander Popp, and Benedikt Schmuelling. 2021. "Analysis of Cell-to-Cell Variation in a Battery Pack after Long Service Life Using Parameter Identification." In *2021 IEEE 4th International Conference on Power and Energy Applications (ICPEA)*, 38–42. Busan, Korea, Republic of: IEEE. <https://doi.org/10.1109/ICPEA52760.2021.9639370>.
- Tian, Jinpeng, Rui Xiong, Weixiang Shen, and Fengchun Sun. 2021. "Electrode Ageing Estimation and Open Circuit Voltage Reconstruction for Lithium Ion Batteries." *Energy Storage Materials* 37 (May): 283–95. <https://doi.org/10.1016/j.ensm.2021.02.018>.
- Tomaszewska, Anna, Zhengyu Chu, Xuning Feng, Simon O'Kane, Xinhua Liu, Jingyi Chen, Chenzhen Ji, et al. 2019. "Lithium-Ion Battery Fast Charging: A Review." *ETransportation* 1 (August): 100011. <https://doi.org/10.1016/j.etrans.2019.100011>.
- Trentadue, Germana, Alexandre Lucas, Marcos Otura, Konstantinos Pliakostathis, Marco Zanni, and Harald Scholz. 2018. "Evaluation of Fast Charging Efficiency under Extreme Temperatures." *Energies* 11 (8): 1937. <https://doi.org/10.3390/en11081937>.
- Zhu, Juner, Ian Mathews, Dongsheng Ren, Wei Li, Daniel Cogswell, Bobin Xing, Tobias Sedlatschek, et al. 2021. "End-of-Life or Second-Life Options for Retired Electric Vehicle Batteries." *Cell Reports Physical Science* 2 (8): 100537. <https://doi.org/10.1016/j.xcrp.2021.100537>.